

# Stable and “bounded excursion” gravastars, and black holes in Einstein’s theory of gravity

P. Rocha <sup>1,3,\*</sup> R. Chan <sup>2,†</sup> M.F.A. da Silva <sup>1,‡</sup> and Anzhong Wang <sup>1,4§</sup>

<sup>1</sup> *Departamento de Física Teórica, Instituto de Física,  
Universidade do Estado do Rio de Janeiro, Rua São Francisco Xavier 524,  
Maracanã 20550-900, Rio de Janeiro - RJ, Brasil*

<sup>2</sup> *Coordenação de Astronomia e Astrofísica,  
Observatório Nacional, Rua General José Cristino, 77,  
São Cristóvão 20921-400, Rio de Janeiro, RJ, Brazil*

<sup>3</sup> *Universidade Estácio de Sá, Rio de Janeiro, RJ, Brazil*

<sup>4</sup> *GCAP-CASPER, Department of Physics,  
Baylor University, Waco, TX 76798, USA*

Dynamical models of prototype gravastars are constructed and studied. The models are the Visser-Wiltshire three-layer gravastars, in which an infinitely thin spherical shell of a perfect fluid with the equation of state  $p = (1 - \gamma)\sigma$  divides the whole spacetime into two regions, where the internal region is de Sitter, and the external is Schwarzschild. When  $\gamma < 1$  and  $\Lambda \neq 0$ , it is found that in some cases the models represent stable gravastars, and in some cases they represent “bounded excursion” stable gravastars, where the thin shell is oscillating between two finite radii, while in some other cases they collapse until the formation of black holes. However, when  $\gamma \geq 1$ , even with  $\Lambda \neq 0$ , only black holes are found. In the phase space, the region for both stable gravastars and “bounded excursion” gravastars is very small in comparison to that of black holes, although it is not completely empty.

PACS numbers: 98.80.-k,04.20.Cv,04.70.Dy

---

\*Electronic address: pedroennarocho@gmail.com

†Electronic address: chan@on.br

‡Electronic address: mfasnic@gmail.com

§Electronic address: anzhong.wang@baylor.edu

## I. INTRODUCTION

As alternatives to black holes, gravastars have received some attention recently [1], partially due to the tight connection between the cosmological constant and a currently accelerating universe [2], although very strict observational constraints on the existence of such stars may exist [3]. In the original model of Mazur and Mottola (MM) [4], gravastars consist of five layers: an internal core  $0 < r < r_1$ , described by the de Sitter universe, an intermediate thin layer of stiff fluid  $r_1 < r < r_2$ , and an external region  $r > r_2$ , described by the Schwarzschild solution,

$$ds^2 = -f(r)dt^2 + \frac{1}{f(r)}dr^2 + r^2(d\theta^2 + \sin^2\theta d\varphi^2), \quad (1.1)$$

where the function  $f(r)$  is given by  $f(r) = 1 - 2\mathcal{M}/r$ , in the units where  $c = 1 = G$ . In addition, in such a setup, two infinitely thin shells also appear, respectively, on the hypersurfaces  $r = r_1$  and  $r = r_2$ . By properly choosing the free parameters involved, one can show that the two shells can have only tensions but with opposite signs [4]. Visser and Wiltshire (VW) argued that such five-layer models can be simplified to three-layer ones [5], in which the two infinitely thin shells and the intermediate region are replaced by one infinitely thin shell, so that the function  $f(r)$  in the metric (1.1) is given by

$$f(r) = \begin{cases} 1 - \frac{2\mathcal{M}}{r}, & r > a(\tau), \\ 1 - \left(\frac{r}{l}\right)^2, & r < a(\tau), \end{cases} \quad (1.2)$$

where  $r = a(\tau)$  is a timelike hypersurface, at which the infinitely thin shell is located, and  $\tau$  denotes the proper time of the thin shell. The constant  $l \equiv \sqrt{3/\Lambda}$  denotes the de Sitter radius. On the hypersurface  $r = a(\tau)$  Israel junction conditions yield

$$\frac{1}{2}\dot{a}^2 + V(a) = 0, \quad (1.3)$$

where an overdot denotes the derivative with respect to the proper time  $\tau$  of the thin shell. Therefore, in the region  $r > a(\tau)$  the spacetime is locally Schwarzschild, while in the region  $r < a(\tau)$  it is locally de Sitter. These two different regions are connected through a dynamical infinitely thin shell located at  $r = a(\tau)$  to form a new spacetime of gravastar.

Two different types of stable gravastars are identified by VW, stable gravastars and “bounded excursion” gravastars.

**Stable gravastars:** In this case, there must exist a radius  $a_0$  such that

$$V(a_0) = 0, \quad V'(a_0) = 0, \quad V''(a_0) > 0, \quad (1.4)$$

where a prime denotes the ordinary differentiation with respect to the indicated argument. If and only if there exists such an  $a_0$  for which the above conditions are satisfied, the model is said to be stable. Among other things, VW found that there are many equations of state for which the gravastar configurations are stable, while others are not [5]. Carter studied the same problem and found new equations of state for which the gravastar is stable [6], while De Benedictis *et al* [7] and Chirenti and Rezzolla [8] investigated the stability of the original model of Mazur and Mottola against axial-perturbations, and found that gravastars are stable to these perturbations. Chirenti and Rezzolla also showed that their quasi-normal modes differ from those of a black hole of the same mass, and thus can be used to discern a gravastar from a black hole. Early work on dynamical thin shells with de Sitter interior and (A)dS-RN exterior can be found in [9].

**“Bounded excursion” gravastars:** As VW noticed, there is a less stringent notion of stability, the so-called “bounded excursion” models, in which there exist two radii  $a_1$  and  $a_2$  such that

$$V(a_1) = 0, \quad V'(a_1) \leq 0, \quad V(a_2) = 0, \quad V'(a_2) \geq 0, \quad (1.5)$$

with  $V(a) < 0$  for  $a \in (a_1, a_2)$ , where  $a_2 > a_1$ .

Lately, we studied this type of gravastars [10], and found that, among other things, such configurations can indeed be constructed, although the region for the formation of this type of gravastars is very small in comparison to that of black holes.

In this paper, we generalize our previous work [10] to the case where the equation of state of the infinitely thin shell is given by  $p = (1 - \gamma)\sigma$  with  $\gamma$  being a constant. When  $\gamma = 0$  it reduces to the case we studied in [10]. We shall first construct three-layer dynamical models, in analogy to the VW models, and then show both stable gravastars of the both types and black holes exist for  $\gamma < 1$  and  $\Lambda \neq 0$ . However, when  $\gamma \geq 1$  even with  $\Lambda \neq 0$ , only black holes are found. In the phase space, the region of gravastars and the one of black holes are non-zero, although the former is much smaller than the latter. The rest of the paper is organized as follows: In Sec. II we shall study various cases, in which all the possibilities of forming black holes, gravastars, de Sitter, and Minkowski spacetime exist. In Sec. III we present our main conclusions.

## II. FORMATION OF GRAVASTARS AND BLACK HOLES FROM GRAVITATIONAL COLLAPSE OF PROTOTYPE GRAVASTARS

For spacetimes given by,

$$ds^2 = \begin{cases} c_- (-c_- f_- dv_- + 2dr_-) dv_- + r_-^2 d^2\Omega, & r < a(\tau), \\ c_+ (-c_+ f_+ dv_+ + 2dr_+) dv_+ + r_+^2 d^2\Omega, & r > a(\tau), \end{cases} \quad (2.1)$$

Lake found that the Israel's junction conditions yield two independent equations [11],

$$\dot{a}^2 = \left(\frac{a}{2M}\right)^2 (f_+ - f_-)^2 - \frac{1}{2}(f_+ + f_-) + \left(\frac{M}{2a}\right)^2, \quad (2.2)$$

$$\dot{M} + 8\pi a \dot{a} p = 4\pi a^2 [T_{\alpha\beta} u^\alpha n^\beta], \quad (2.3)$$

where  $M \equiv 4\pi a^2 \sigma$ ,  $\sigma$  denotes the energy density of the shell, and  $p$  its pressure. In this work, we shall consider the case where inside the shell the spacetime is de Sitter, and outside it is Schwarzschild, namely

$$f_+(r) = 1 - \frac{2\mathcal{M}}{r}, \quad f_-(r) = 1 - \left(\frac{r}{l}\right)^2, \quad (2.4)$$

as that studied in [10]. The only difference is the equation of state of the thin shell, where in the present paper we consider a more general case in which it is taken as,

$$p = (1 - \gamma)\sigma, \quad (2.5)$$

with  $\gamma$  being a constant. When  $\gamma = 0$  it reduces to the special case studied in [10]. Since

$$T_{\mu\nu}^+ = 0, \quad T_{\mu\nu}^- = \Lambda g_{\mu\nu}^-, \quad (2.6)$$

we find

$$[T_{\mu\nu} u^\mu n^\nu] = T_{\mu\nu}^+ u^{+\mu} n^{+\nu} - T_{\mu\nu}^- u^{-\mu} n^{-\nu} = 0. \quad (2.7)$$

Then, from (2.3) we find

$$\frac{\dot{\sigma}}{\sigma} = -2(2 - \gamma)\frac{\dot{a}}{a}, \quad (2.8)$$

which has the general solution,

$$\sigma = \sigma_0 \left(\frac{a_0}{a}\right)^{2(2-\gamma)}. \quad (2.9)$$

Setting

$$\mathcal{M} = mL_0, \quad a(\tau) = R(\tau)L_0, \quad l = LL_0, \quad (2.10)$$

where

$$L_0 \equiv \left(4\pi\sigma_0 a_0^{2(2-\gamma)}\right)^{-\frac{1}{2\gamma-3}}, \quad (2.11)$$

we find that Eq.(2.2) can be cast in the form,

$$\frac{1}{2}R^{*2} + V(R, m, L, \gamma) = 0, \quad (2.12)$$

where  $R^* \equiv dR/d(L_0^{-1}\tau)$ , and

$$V(R, m, L, \gamma) = -\frac{1}{2} \left\{ -1 + \frac{m}{R} + \frac{1}{4}R^{4\gamma-6} + m^2 R^{4(1-\gamma)} + \frac{R^2}{2L^2} - \frac{mR^{7-4\gamma}}{L^2} + \frac{R^{10-4\gamma}}{4L^4} \right\}. \quad (2.13)$$

Therefore, for any given constants  $m$ ,  $L$  and  $\gamma$ , Eq.(2.12) uniquely determines the collapse of the prototype gravastar. Depending on the initial value  $R_0$ , the collapse can form either a black hole, or gravastar, or a Minkowski, or a de Sitter space. In the last case, the thin shell first collapses to a finite non-zero minimal radius and then expands to infinity. To guarantee that initially the spacetime does not have any kind of horizons, cosmological or event, we must restrict  $R_0$  to the range,

$$2m < R_0 < L, \quad (2.14)$$

correspondingly  $a_0 \in (2\mathcal{M}, l)$ . When  $m = 0 = \Lambda$ , the thin shell disappears, and the whole spacetime is Minkowski. So, in the following we shall not consider this case.

From Eq.(2.13), we find that

$$\begin{aligned} \frac{\partial V(R, m, L, \gamma)}{\partial R} &= \frac{m}{2} \left( \frac{1}{R^2} + (7-4\gamma) \frac{R^{6-4\gamma}}{L^2} \right) - 2m^2 (1-\gamma) R^{3-4\gamma} - \frac{R}{2L^2} \\ &\quad + \frac{1}{4} (3-2\gamma) R^{4\gamma-7}. \end{aligned} \quad (2.15)$$

As both equations,  $V = 0$  and  $\partial V(R, m, L, \gamma)/\partial R = 0$ , are quadratic in  $m$ , we can easily find  $m$  from these two equations, which is given by

$$\begin{aligned} m_c(R, L, \gamma) &= \frac{1}{2L^2 (-5L^2 R^{4\gamma} + 4L^2 \gamma R^{4\gamma} - 3R^8)} (-8R^{4\gamma+1}L^4 + 8R^{4\gamma+1}L^4\gamma \\ &\quad - 3R^{11} - 4R^{8\gamma-5}L^4\gamma + 5R^{8\gamma-5}L^4 \\ &\quad + 2R^{4\gamma+3}L^2 - 4R^{4\gamma+3}L^2\gamma), \quad (V = V' = 0). \end{aligned} \quad (2.16)$$

Substituting this expression in  $V = 0$  we find six functions  $L(R, \gamma)$ . Due to the complexity of these expressions we shall not give them here explicitly. Instead, in the following we consider some particular cases.

**A.**  $m = 0$

In this case, the spacetime outside the thin shell is flat, and the mass of the shell completely screens the mass of the internal de Sitter spacetime. From Eq.(2.13) we find that

$$V(R, L, \gamma) = -\frac{1}{2} \left\{ -1 + \frac{1}{4} R^{4\gamma-6} + \frac{R^2}{2L^2} + \frac{R^{10-4\gamma}}{4L^4} \right\}. \quad (2.17)$$

Then,  $V'(R) = 0$  yields,

$$(2\gamma - 3) L^4 + 2R^{4(2-\gamma)} L^2 - (2\gamma - 5) R^{8(2-\gamma)} = 0, \quad (2.18)$$

which has real solution only for  $\gamma < 3/2$  or  $\gamma \geq 5/2$ , and the corresponding solution is given by

$$L_c = \left| \frac{2\gamma - 5}{2\gamma - 3} \right|^{1/2} R_c^{2(2-\gamma)}, \quad \gamma \notin [3/2, 5/2). \quad (2.19)$$

Substituting the above expression into the equation  $V(R) = 0$ , we find

$$R_c = \left| \frac{2(\gamma - 2)}{2\gamma - 5} \right|^{\frac{1}{3-2\gamma}}. \quad (2.20)$$

Figs. 1 and 2, and Table I show the functions of  $R_c(\gamma)$  and  $L_c(\gamma)$ , where for  $\gamma \in [3/2, 5/2)$ , the equations  $V(R, L, \gamma) = 0$  and  $V'(R, L, \gamma) = 0$  have no real solutions. In particular, when  $\gamma = 0.5$  we find that  $L_c \approx 0.9185586537$  and  $R_c \approx 0.8660254039$ . For  $L < L_c$  the potential is strictly negative as shown in Fig. 3. Thus, if the star starts to collapse at  $R = R_0$ , it will collapse continuously until  $R = 0$ , whereby a Minkowski spacetime is formed. When  $L = L_c$ , since  $R_0 < L_c$ , we can see that, the star will collapse until the center and turns the whole spacetime into a Minkowski. For  $L > L_c$ , the potential  $V(R)$  is positive between  $R_1$  and  $R_2$ , where  $R_{1,2}$  are the two real roots of the equation  $V(R, L > L_c) = 0$  with  $R_2 > R_1 > 0$ . In this case, if the star starts to collapse with  $R_0 < R_1$ , as can be seen from Fig. 3, it will collapse to  $R = 0$  whereby a Minkowski spacetime is finally formed. If it starts to collapse with  $R_0 > R_2$ , it will first collapse to  $R = R_2$  and then starts to expand until  $R = \infty$ , and the whole spacetime is finally de Sitter.

It should be noted that in this case we always have  $V''(R_c, L_c, \gamma) < 0$ , that is, no stable stars exist.

TABLE I: Some values of  $R_c$  and  $L_c$  as a function of  $\gamma$  for  $\Lambda \neq 0$  and  $m = 0$ .

$\gamma$	$R_c$	$L_c$
0.0	0.9283177667	0.9587624669
0.1	0.9199519160	0.9535623390
0.2	0.9100298584	0.9473109395
0.3	0.8981404718	0.9397043233
0.4	0.8837277541	0.9303202778
0.5	0.8660254039	0.9185586537
0.6	0.8439546889	0.9035435931
0.7	0.8159607706	0.8839575014
0.8	0.7797433156	0.8577474304
0.9	0.7318025503	0.8215821352
1.0	0.6666666667	0.7698003592
1.1	0.5756295655	0.6922956261
1.2	0.4452231361	0.5703420705
1.3	0.2598914458	0.3713508347
1.4	0.0482828420	0.08734694771
2.6	0.4428889922	0.8012163331
2.7	0.5933418502	0.8478077860
2.8	0.6857500883	0.8784631649
2.9	0.7485495080	0.9002622198
3.0	0.7937005260	0.9164864251
5.0	0.9742903329	0.9881107444

### B. $\Lambda = 0$

In this case, Eq.(2.13) reduces to

$$V(R, m, \gamma) = \frac{1}{8R^6} (4R^6 - 4mR^5 - R^{4\gamma} - 4R^{10-4\gamma}m^2), \quad (2.21)$$

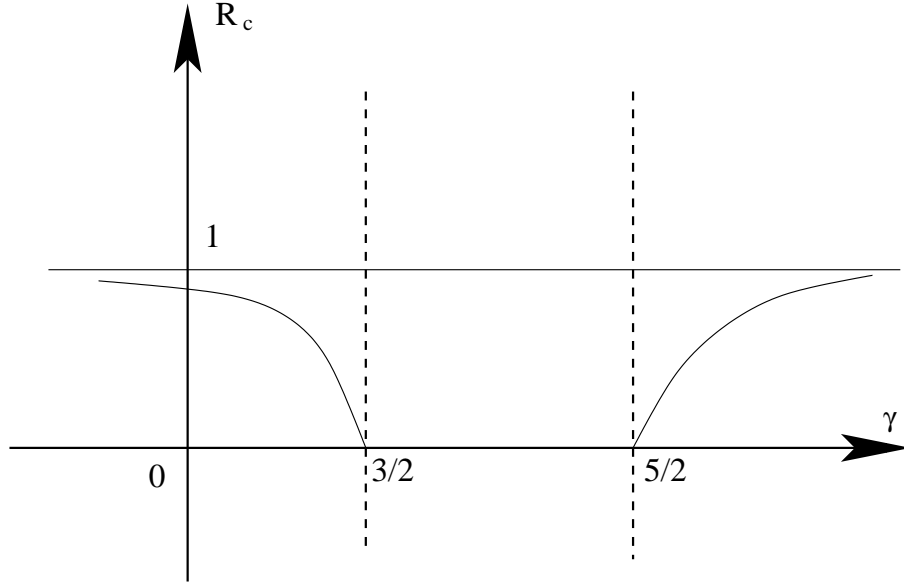


FIG. 1: The function  $R_c$  defined in Eq.(2.18) for  $m = 0$ .

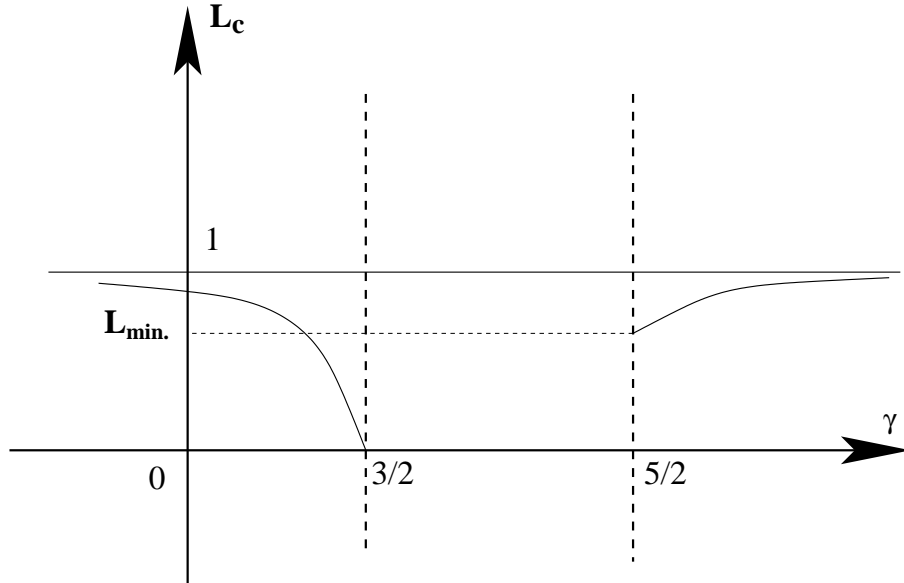


FIG. 2: The function  $L_c$  defined in Eq.(2.19) for  $m = 0$ , where  $L_{min} = 1/\sqrt{2}$ .

from which we find that the equations  $V(R) = 0$  and  $V'(R) = 0$  have the explicit solutions,

$$R_c(\gamma) = \left| \frac{4 - 4\gamma}{5 - 4\gamma} \right|^{\frac{1}{(2\gamma-3)}}, \quad (2.22)$$

$$m_c = \frac{1}{2} \sqrt{R_c^{2(4\gamma-5)} + \frac{4}{5-4\gamma} R_c^{4\gamma-4}}. \quad (2.23)$$

Figs. 4 and 5 show the dependence of  $R_c$  and  $m_c$  on  $\gamma$ . The results of our previous work



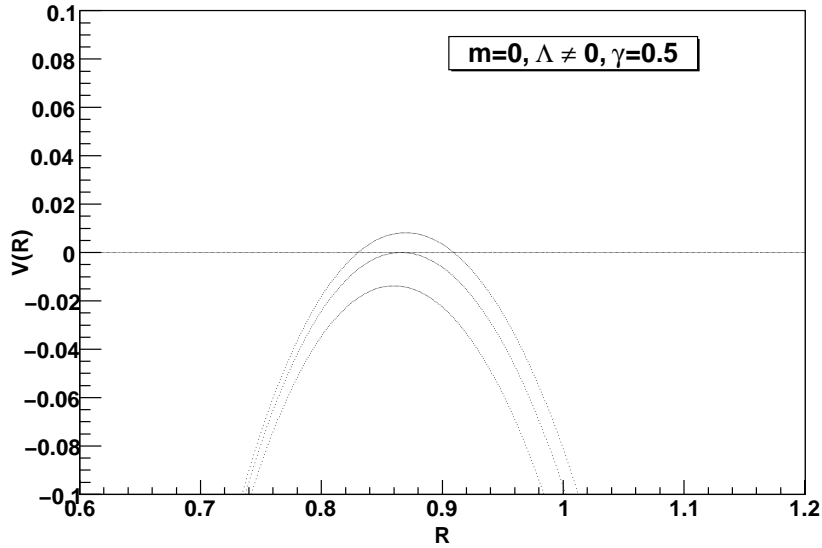


FIG. 3: The potential  $V(R)$  for  $m = 0$  and  $\gamma = 0.5$ . The top line is for  $L > L_c$ , the middle line is for  $L = L_c$ , and the bottom line is for  $L < L_c$ .

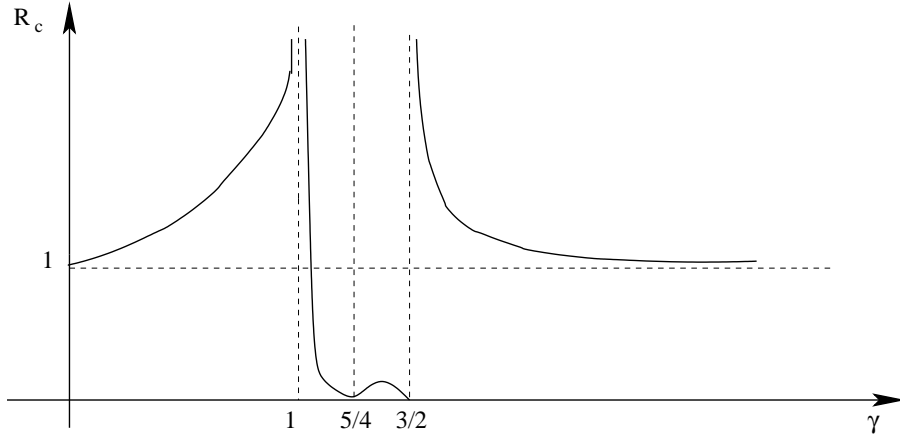


FIG. 4: The function  $R_c$  defined in Eq.(2.22) for  $\Lambda = 0$ .

are obtained when  $\gamma = 0$  [10]. Some representative cases are  $\gamma = 0.5$  and  $\gamma = 3.0$ . For  $\gamma = 0.5$ , we find that  $m_c \approx 0.5443310540$  and  $R_c \approx 1.224744871$ , and for  $\gamma = 3.0$  we find that  $m_c \approx 0.5120894280$  and  $R_c \approx 1.045515917$ . In both cases, for  $m > m_c$  the potential  $V(R)$  is strictly negative as shown in Figs. 6 and 7. Then, the collapse always forms black holes. For  $m = m_c$ , there are two different possibilities, depending on the choice of the initial radius  $R_0$ . In particular, if the star begins to collapse with  $R_0 > R_c$ , the collapse will asymptotically approach the minimal radius  $R_c$ . Once it collapses to this point, the shell

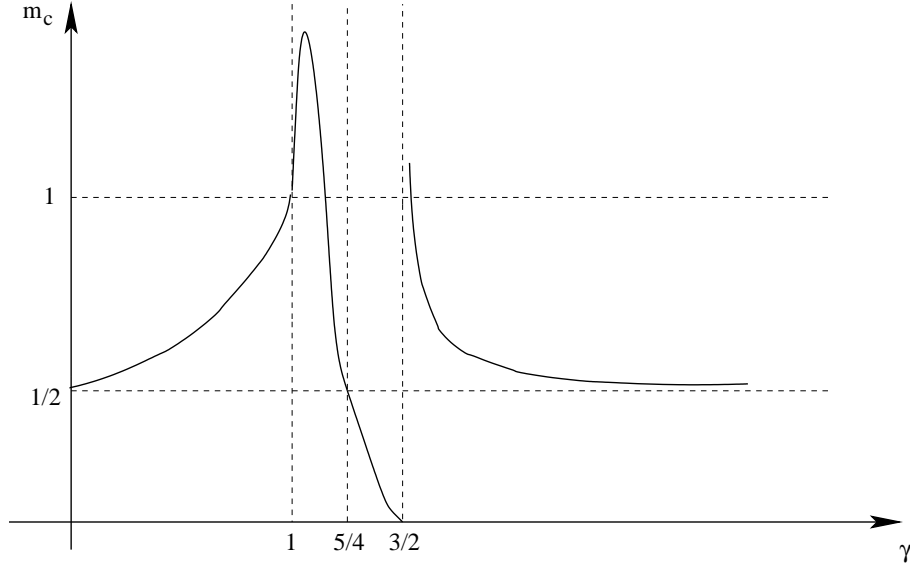


FIG. 5: The function  $m_c$  defined in Eq.(2.23) for  $\Lambda = 0$ .

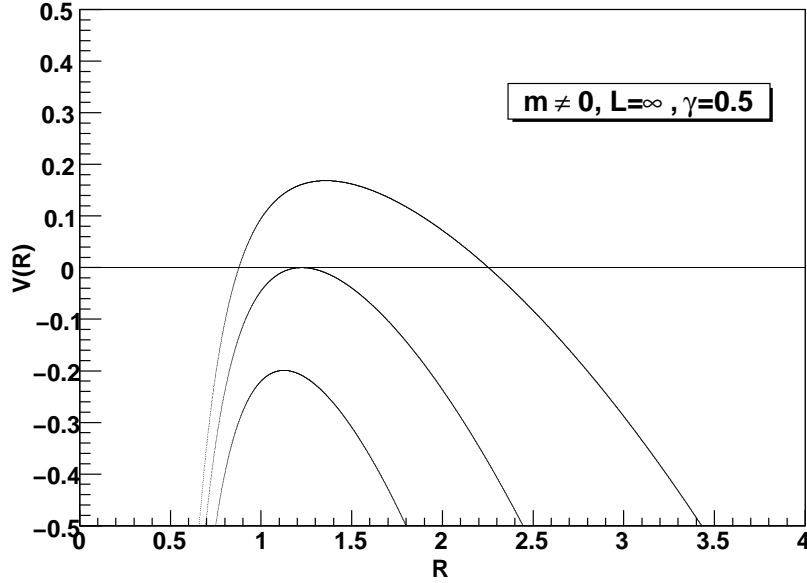


FIG. 6: The potential  $V(R)$  for  $\gamma = 0.5$ . The top line is for  $m < m_c$ , the middle line is for  $m = m_c$ , and the bottom line is for  $m > m_c$ .

will stop collapsing and remains there for ever. However, in this case this point is unstable and any small perturbations will lead the star either to expand for ever and leave behind a flat spacetime, or to collapse until  $R = 0$ , whereby a Schwarzschild black hole is finally formed. On the other hand, if the star begins to collapse with  $2m_c < R_0 < R_c$  as shown in

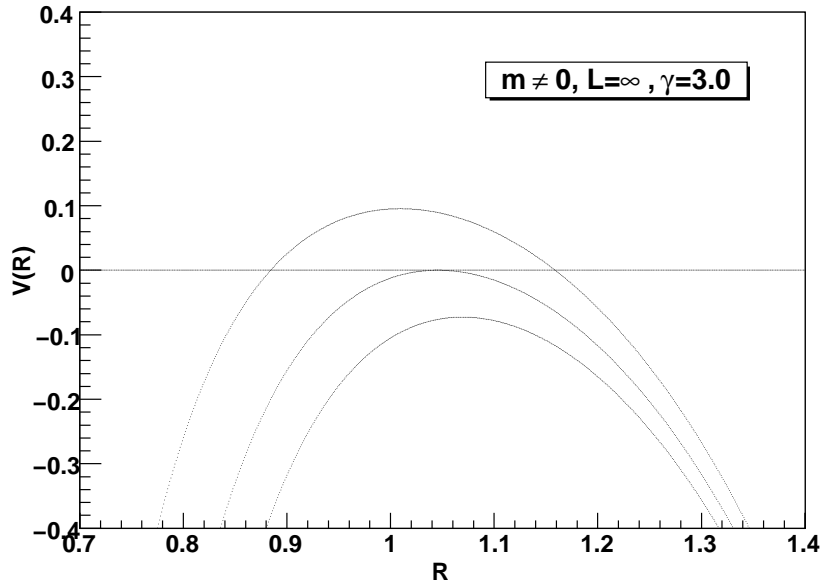


FIG. 7: The potential  $V(R)$  for  $\gamma = 3.0$ . The top line is for  $m < m_c$ , the middle line is for  $m = m_c$ , and the bottom line is for  $m > m_c$ .

Figs. 6 and 7, the star will collapse until a black hole is formed. For  $m < m_c$ , the potentials  $V(R)$  for each case have a positive maximal, and the equation  $V(R, m < m_c) = 0$  has two positive roots  $R_{1,2}$  with  $R_2 > R_1 > 0$ . There are two possibilities here, depending on the choice of the initial radius  $R_0$ . If  $R_0 > R_2$ , the star will first collapse to its minimal radius  $R = R_2$  and then expand to infinity, whereby a Minkowski spacetime is finally formed. If  $2m < R_0 < R_1$ , the star will collapse continuously until  $R = 0$ , and a black hole will be finally formed.

It should be noted that, similar to the last case, now we always have  $V''(R_c, m_c, \gamma) < 0$ , which means that no stable stars exist in this case, too.

### C. $m \neq 0$ and $\Lambda \neq 0$

As mentioned before, the analytic expression for  $L_c$  in the present case are too complicated to write out here. Instead, we shall study it numerically. Our main strategy is to start with  $m_c$  obtained for the case  $\Lambda = 0$ , and then gradually turn on  $\Lambda$ . We plot the potential  $V(R, m_c(\gamma), L, \gamma)$  as a function of  $R$  for any given  $\gamma$ , by finely tuning  $L$  until a stable gravastar or a bounded excursion gravastar is found [see Figs. 8-11]. The value  $L_c$ , as shown

TABLE II: Some values of  $R_c$  and  $m_c$  as a function of  $\gamma$  for  $\Lambda = 0$  and  $m \neq 0$ 

$\gamma$	$R_c$	$m_c$
0.0	1.077217345	0.5170643255
0.1	1.091490000	0.5199536485
0.2	1.110255191	0.5236577775
0.3	1.135692224	0.5285215890
0.4	1.171542463	0.5350989795
0.5	1.224744871	0.5443310540
0.6	1.309606309	0.5579387820
0.7	1.460581840	0.5794043665
0.8	1.784674184	0.6169244095
0.9	2.840468889	0.6956250340
1.0	$\infty$	1.000000000
1.1	1.475575893	1.660022879
1.2	0.09921256570	1.190550789
1.3	0.01134023029	0.1360827636
1.4	0.007415771480	0.006591796870
1.5	Undefined	Undefined
1.6	3.625777848	14.80525970
1.7	3.017962339	1.043246245
1.8	1.867291683	0.7407438105
1.9	1.501970633	0.6398928165
2.0	1.333333333	0.5925925920
3.0	1.045515917	0.5120894280
4.0	1.017554577	0.5045725165
$1.0 \times 10^5$	1.000000000	0.500000000

in Table III, is obtained numerically when a stable gravastar is found for a specific pair  $(m_c, \gamma)$ .

It can be shown that both types of gravastars can be formed for  $\gamma \in [0, 1)$ . But for  $\gamma \geq 1$ , we find that for any given values of  $L$  and  $m$  only black holes can be formed, for example,

TABLE III: Some values of  $m_c$  and  $L_c$  obtained numerically as a function of  $\gamma$  in the general case where  $\Lambda \neq 0$  and  $m \neq 0$

$\gamma$	$m_c$	$L_c$
0.0	0.5170643255	2.8743398
0.1	0.5199536485	3.1000618
0.2	0.5236577775	3.3917341
0.3	0.5285215890	3.7828681
0.4	0.5350989795	4.3336020
0.5	0.5443310540	5.1626297
0.6	0.5579387820	6.5372013
0.7	0.5794043665	9.1891232
0.8	0.6169244095	15.8955019
0.9	0.6956250340	47.7590095
0.95	0.7788797565	166.7543222
0.99	0.9200729380	3906.8991705
0.991	0.9259539055	4823.955200
0.992	0.9320895460	6107.378535
0.993	0.9385115510	7981.5666867
0.994	0.9452603485	10873.01788
0.995	0.9523894295	15675.49526
0.996	0.9599731720	24531.28407
0.997	0.9681226815	43701.09808
0.998	0.9770238615	98596.55052
0.999	0.9870615640	395877.877549
0.9999	0.9982370395	$0.3980357873 \times 10^8$
1.7	1.043246242	$0.6064576241 \times 10^8$
3.0	0.5120894280	10410.51705
5.0	0.5023884065	6235.986909

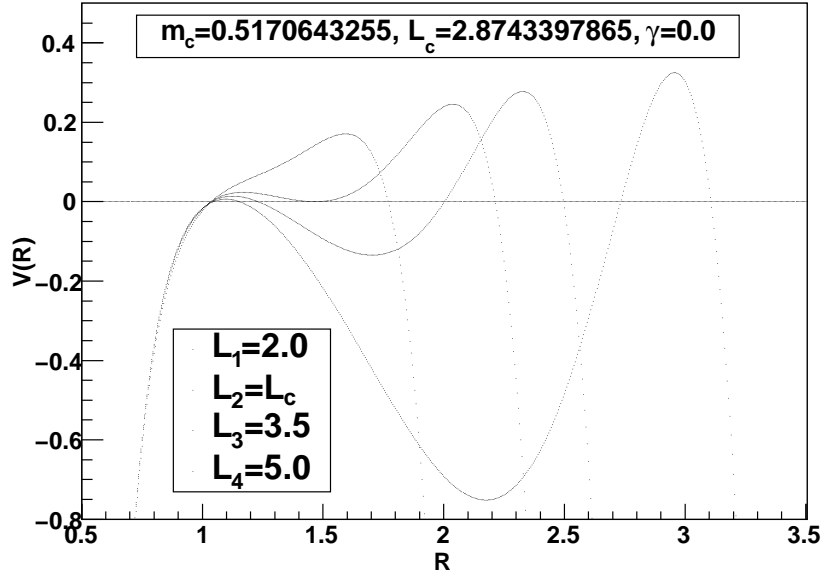


FIG. 8: The potential  $V(R)$  for  $\gamma = 0$  with some values of  $L$  near the critical point  $L = L_c$ . The curves from top to bottom represent  $L_1$  to  $L_4$ , respectively.

see Figs. 19-24. In particular, as  $\gamma \rightarrow 1$ , we find that  $L_c \rightarrow \infty$ . This can be seen from Table III and Figs. 12-18.

In the cases where we can have the two types of stable gravastars, it is also possible to find configurations where black holes are formed. This shows clearly that, even gravastars indeed exist, they do not exclude the existence of black holes.

### III. CONCLUSIONS

In this paper, we have generalized our previous work on the problem of stable gravastars by constructing dynamical three-layer VW models [5], which consists of an internal de Sitter space, a dynamical infinitely thin shell of a perfect fluid with the equation of state  $p = (1 - \gamma)\sigma$ , and an external Schwarzschild spacetime. We have shown explicitly that the final output can be a black hole, a “bounded excursion” gravastar, a stable gravastar, a Minkowski, or a de Sitter spacetime, depending on the total mass  $m$  of the system, the cosmological constant  $\Lambda$ , and the initial position  $R_0$  of the dynamical thin shell. All these possibilities have non-zero measurements in the phase space of  $m$ ,  $\Lambda(\neq 0)$ ,  $\gamma(< 1)$  and  $R_0$ , although the region of gravastars is very small in comparison with that of black holes. When

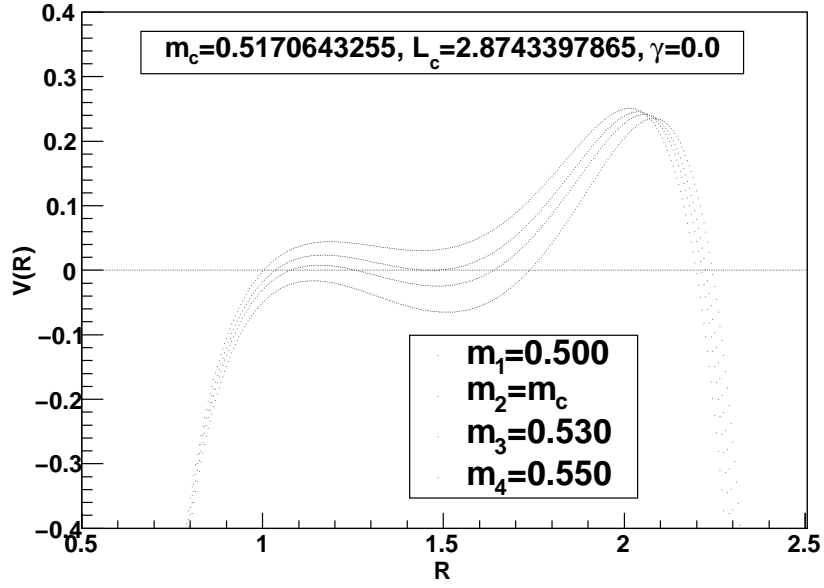


FIG. 9: The potential  $V(R)$  for  $\gamma = 0$  with some values of  $m$  near the critical point  $m = m_c$ . The curves from top to bottom represent  $m_1$  to  $m_4$ , respectively.

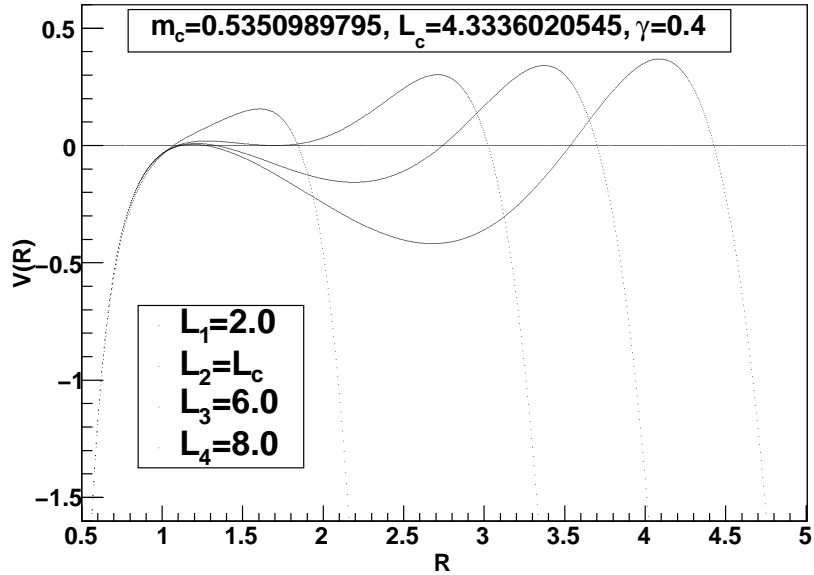


FIG. 10: The potential  $V(R)$  for  $\gamma = 0.4$  with some values of  $L$  near the critical point  $L = L_c$ . The curves from top to bottom represent  $L_1$  to  $L_4$ , respectively.

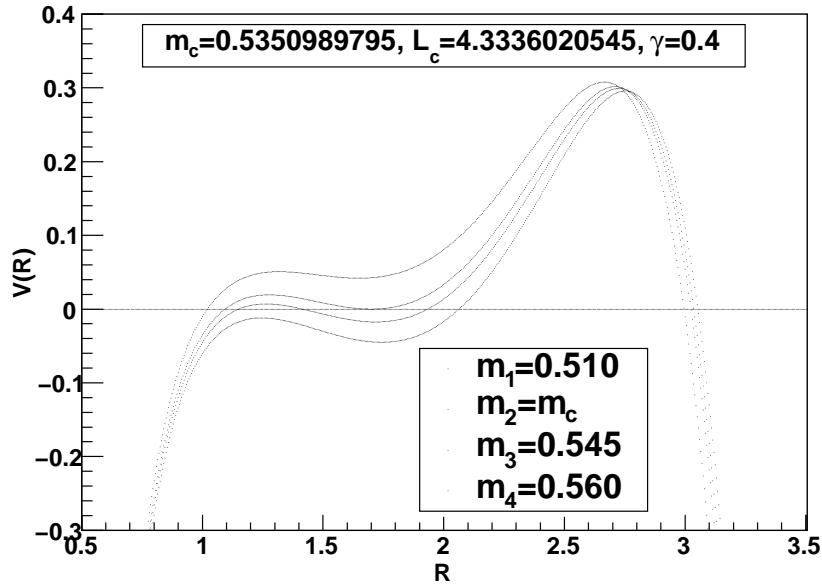


FIG. 11: The potential  $V(R)$  for  $\gamma = 0.4$  with some values of  $m$  near the critical point  $m = m_c$ . The curves from top to bottom represent  $m_1$  to  $m_4$ , respectively.

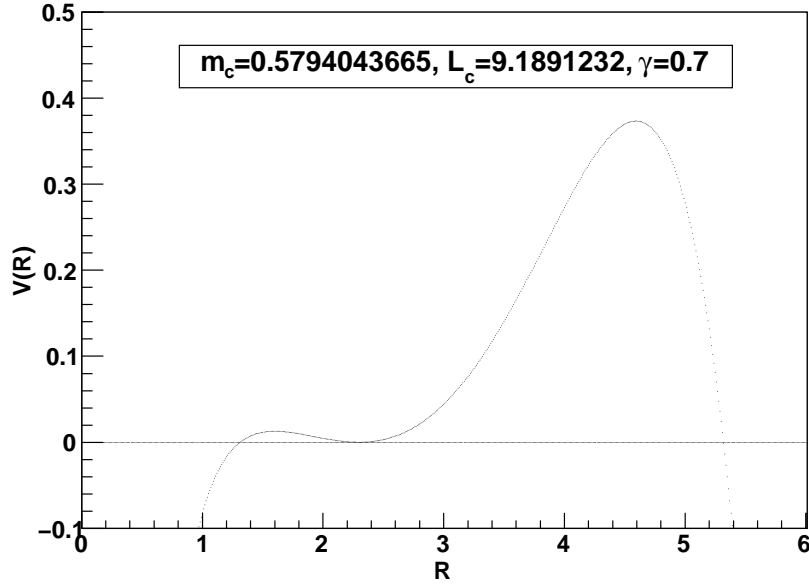
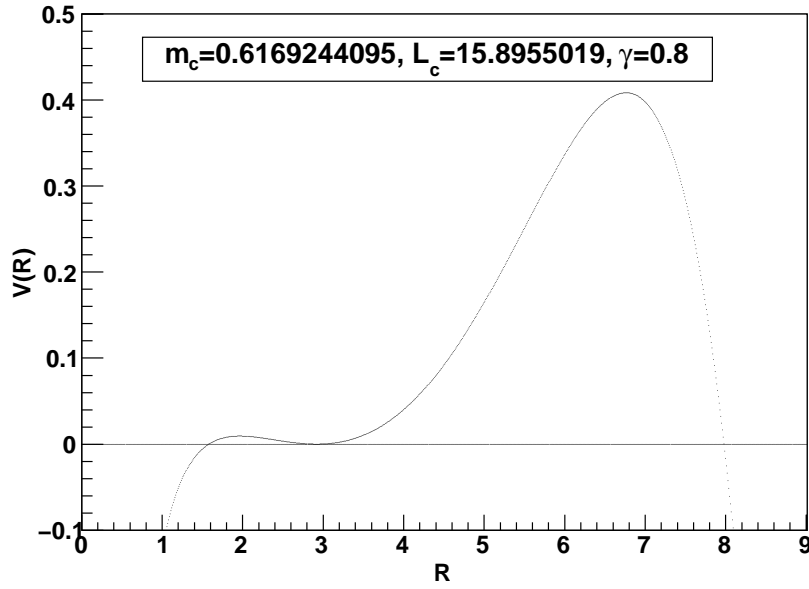
$\gamma \geq 1$  even with  $\Lambda \neq 0$ , only black holes are found. Therefore, although the existence of gravastars cannot be completely excluded in these dynamical models, our results show that, even if gravastars indeed exist, they do not exclude the existence of black holes.

### Acknowledgments

The authors would like to express their gratitude to N.O. Santos for valuable suggestions and discussions. The financial assistance from CNPq (MFAdaS, RC), FAPERJ (MFAdaS, RC), and FINEP (MFAdaS) is gratefully acknowledged.

- 
- [1] C.B.M.H. Chirenti and L. Rezzolla, arXiv:0808.4080; V. Cardoso, P. Pani, M. Cadoni, and M. Cavaglia, arXiv:0808.1615; D. Horvat, S. Ilijic, and A. Marunovic, arXiv:0807.2051; D. Horvat and S. Ilijic, arXiv:0707.1636; P. Marecki, arXiv:gr-qc/0612178; F.S.N. Lobo, Phys. Rev. D **75**, 024023 (2007); arXiv:gr-qc/0612030; Class. Quantum Grav. **23**, 1525 (2006); F.S.N. Lobo, Aaron V. B. Arellano, *ibid.*, **24**, 1069 (2007); T. Faber, arXiv:gr-qc/0607029; C. Cattoen,



FIG. 12: The potential  $V(R)$  for  $\gamma = 0.7$ FIG. 13: The potential  $V(R)$  for  $\gamma = 0.8$ .

arXiv:gr-qc/0606011; O.B. Zaslavskii, Phys. Lett. **B634**, 111 (2006); C. Cattoen, T. Faber, and M. Visser, Class. Quantum Grav. **22**, 4189 (2005).

[2] V. Sahni and A. A. Starobinsky, Int. J. Mod. Phys. D **9**, 373 (2000); P.J.E. Peebles and

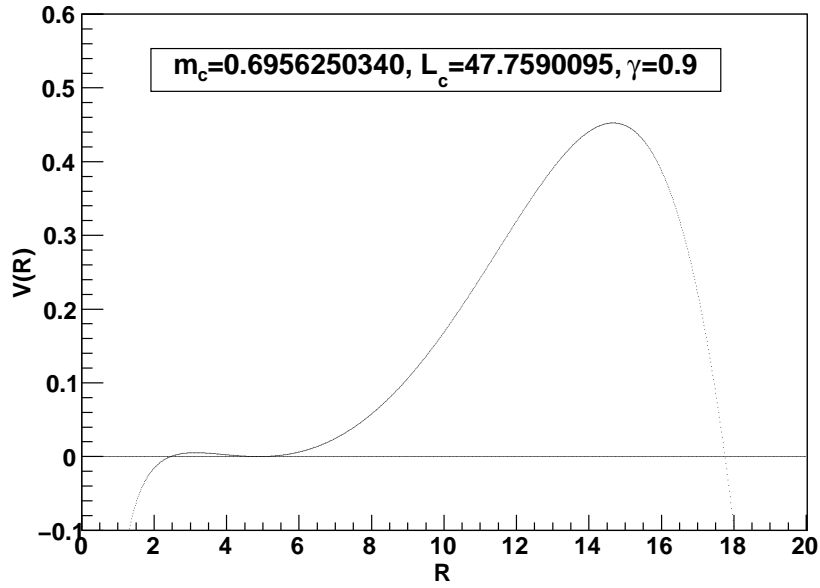


FIG. 14: The potential  $V(R)$  for  $\gamma = 0.9$ .

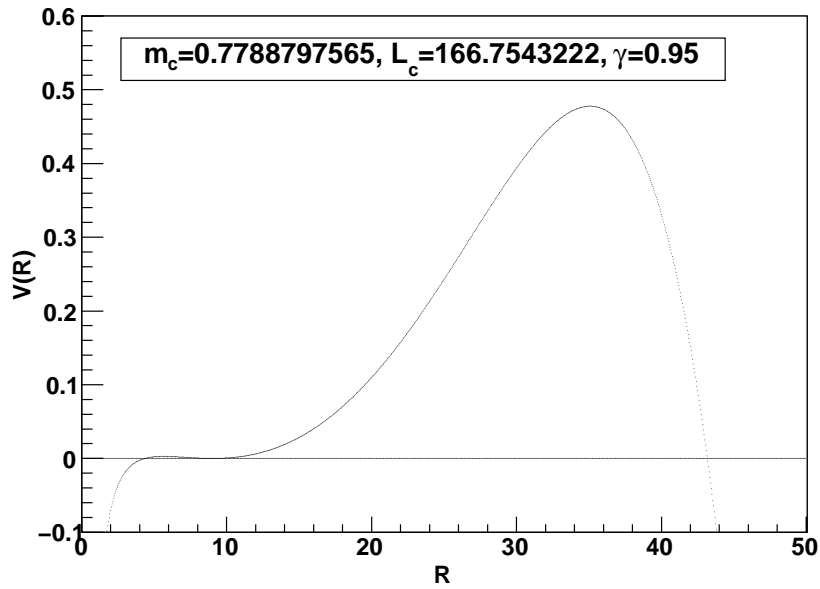


FIG. 15: The potential  $V(R)$  for  $\gamma = 0.95$ .

B. Ratra, *Rev. Mod. Phys.* **75**, 559 (2003); T. Padmanabhan, *Phys. Rep.* **380**, 235 (2003);  
 V. Sahni, “*Dark Matter and Dark Energy*,” arXiv:astro-ph/0403324 (2004); *The Physics of  
 the Early Universe*, edited by E. Papantonopoulos (Springer, New York 2005), P. 141; T.

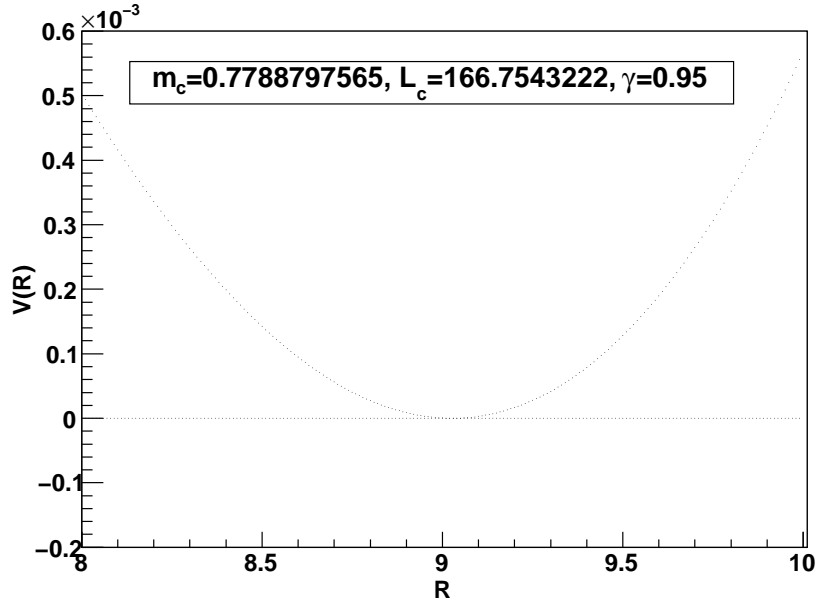


FIG. 16: The potential  $V(R)$  for  $\gamma = 0.95$  near its minimal point.

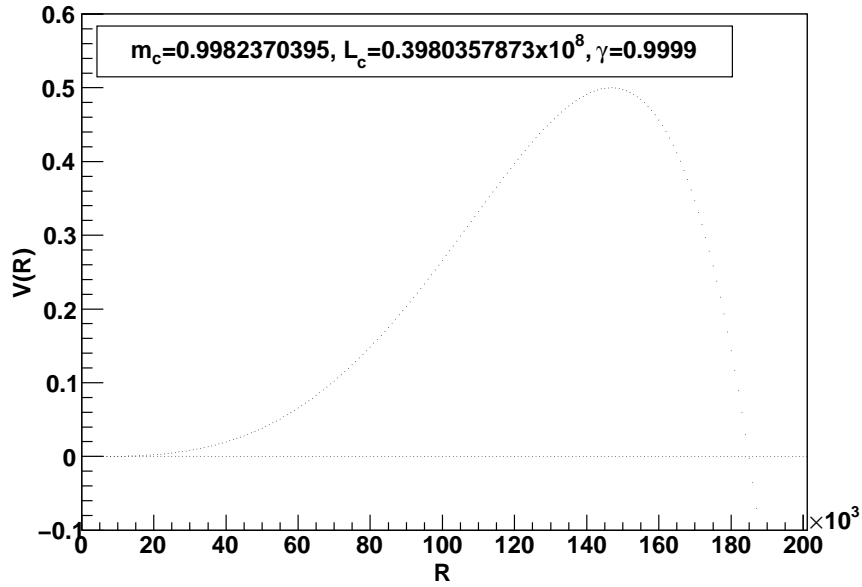


FIG. 17: The potential  $V(R)$  for  $\gamma = 0.9999$

Padmanabhan, Proc. of the 29th Int. Cosmic Ray Conf. **10**, 47 (2005); E.J. Copeland, M. Sami, and S. Tsujikawa, “*Dynamics of dark energy*,” arXiv:hep-th/0603057 (2006); E.W. Kolb, “*Cosmology and the Unexpected*,” arXiv:0709.3102; E. Linder, “*Mapping the cosmolog-*

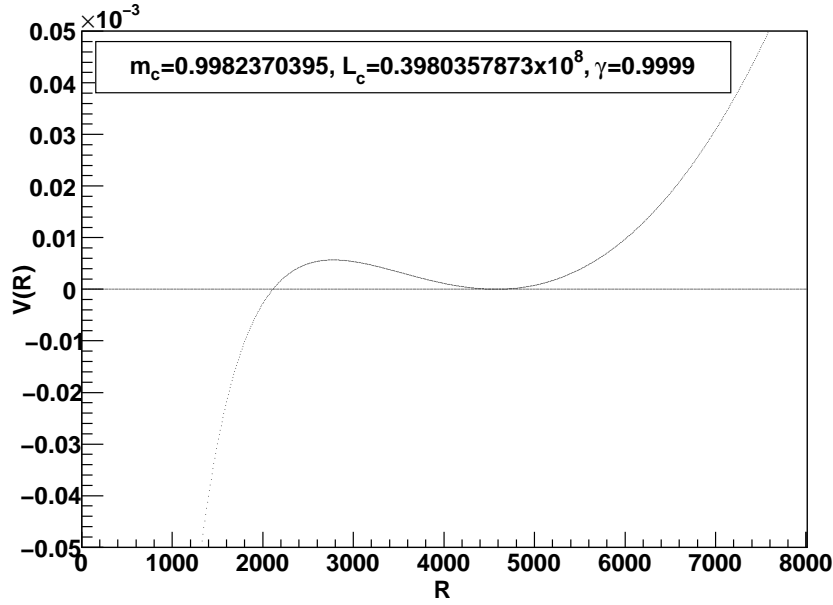


FIG. 18: The potential  $V(R)$  for  $\gamma = 0.9999$  near its minimal point.

*ical expansion,*” arXiv:0801.296; J.A. Frieman, M.S. Turner, and D. Huterer, “*Dark Energy and the Accelerating Universe,*” “*The Dynamics of Collapsing Monopoles and Regular Black Holes,*” arXiv:0803.0982.

- [3] A.E. Broderick and R. Narayan, *Class. Quantum Grav.* **24**, 659 (2007) [arXiv:gr-qc/0701154].
- [4] P.O. Mazur and E. Mottola, “*Gravitational Condensate Stars: An Alternative to Black Holes,*” arXiv:gr-qc/0109035; *Proc. Nat. Acad. Sci.* **101**, 9545 (2004) [arXiv:gr-qc/0407075].
- [5] M. Visser and D.L. Wiltshire, *Class. Quantum Grav.* **21**, 1135 (2004)[arXiv:gr-qc/0310107].
- [6] B.M.N. Carter, *Class. Quantum Grav.* **22**, 4551 (2005) [arXiv:gr-qc/0509087].
- [7] A. DeBenedictis, *et al*, *Class. Quantum Grav.* **23**, 2303 (2006) [arXiv:gr-qc/0511097].
- [8] C.B.M.H. Chirenti and L. Rezzolla, arXiv:0706.1513.
- [9] G.L. Alberghi, D.A. Lowe and M. Trodden, *JHEP*, **9907**, 020 (1999); G. Arreaga, I. Cho, and J. Guven, *Phys. Rev. D***62**, 043520 (2000); H. Cho, D. Kastor, and J.H. Traschen, arXiv:hep-th/0002220.
- [10] P. Rocha, A.Y. Miguelote, R. Chan, M.F. da Silva, N.O. Santos,, and A. Wang, “*Bounded excursion stable gravastars and black holes,*” *J. Cosmol. Astropart. Phys.* **06**, 025 (2008) [arXiv:gr-qc/0803.4200].
- [11] K. Lake, *Phys. Rev. D***19**, 2487 (1979).

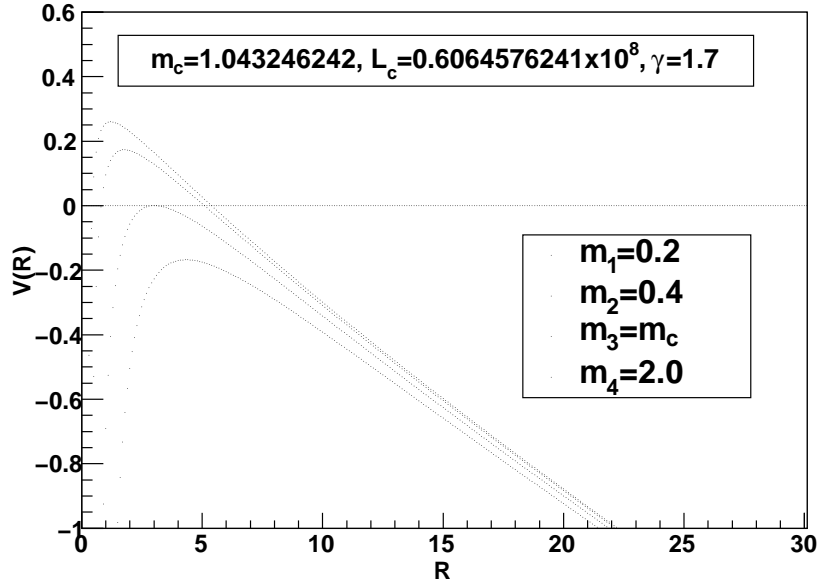


FIG. 19: The potential  $V(R)$  for  $\gamma = 1.7$ . The curves from top to bottom represent  $m_1$  to  $m_4$ , respectively.

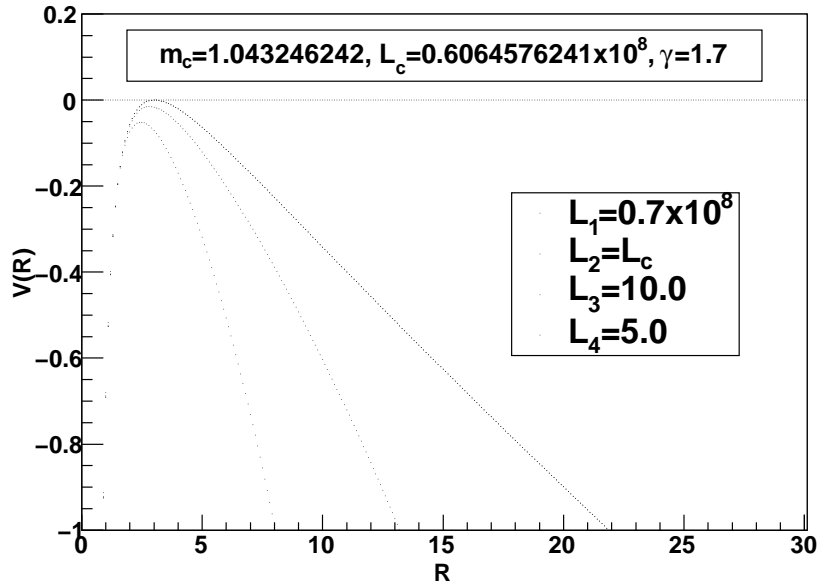


FIG. 20: The potential  $V(R)$  for  $\gamma = 1.7$ . The curves from bottom to top represent  $L_4$  to  $L_1$ , respectively, where the curves  $L_1$  and  $L_2$  coincide. Any potential curve where  $L > L_c$  will coincide with the potential curve where  $L = L_c$

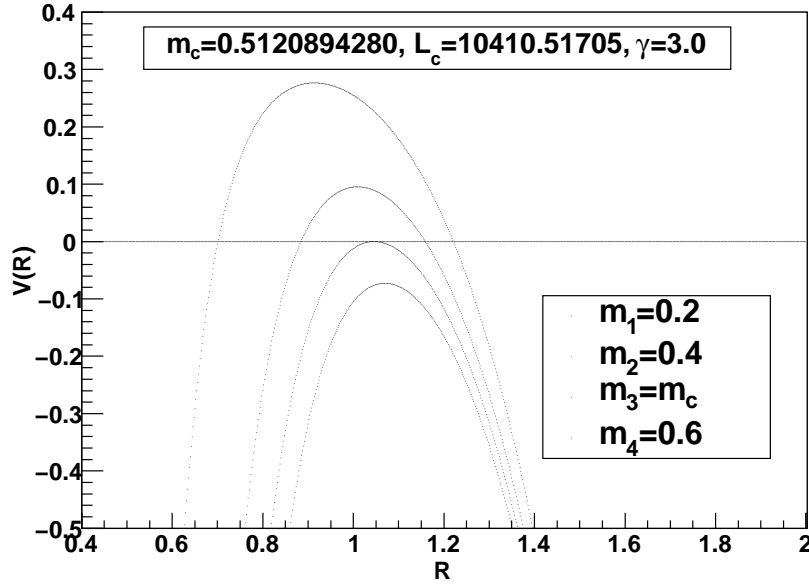


FIG. 21: The potential  $V(R)$  for  $\gamma = 3.0$ . The curves from top to bottom represent  $m_1$  to  $m_4$ , respectively.

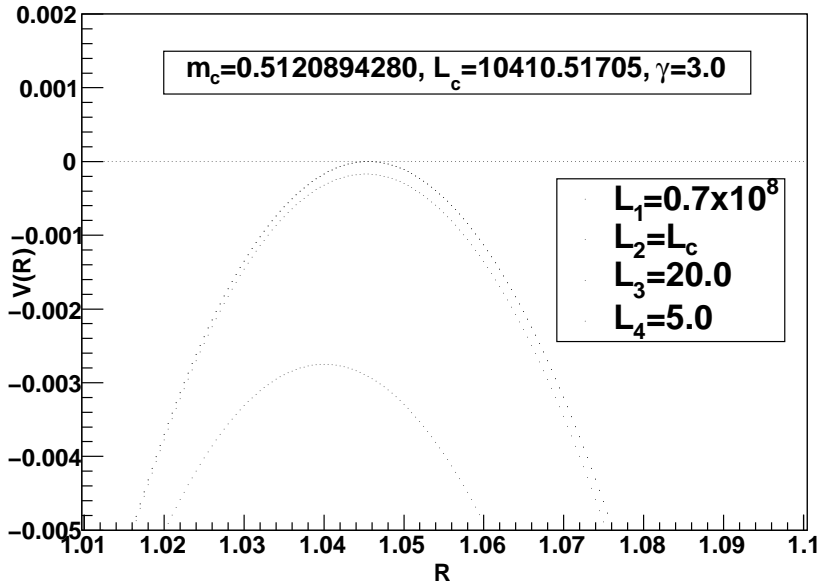


FIG. 22: The potential  $V(R)$  for  $\gamma = 3.0$ . The curves from bottom to top represent  $L_4$  to  $L_1$ , respectively, where the curves  $L_1$  and  $L_2$  coincide. Any potential curve where  $L > L_c$  will coincide with the potential curve where  $L = L_c$ .

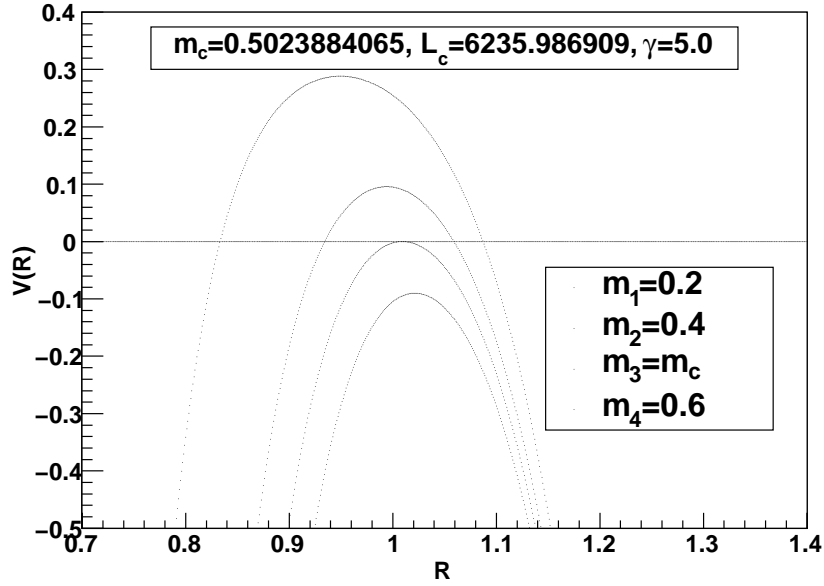


FIG. 23: The potential  $V(R)$  for  $\gamma = 5.0$ . The curves from top to bottom represent  $m_1$  to  $m_4$ , respectively.

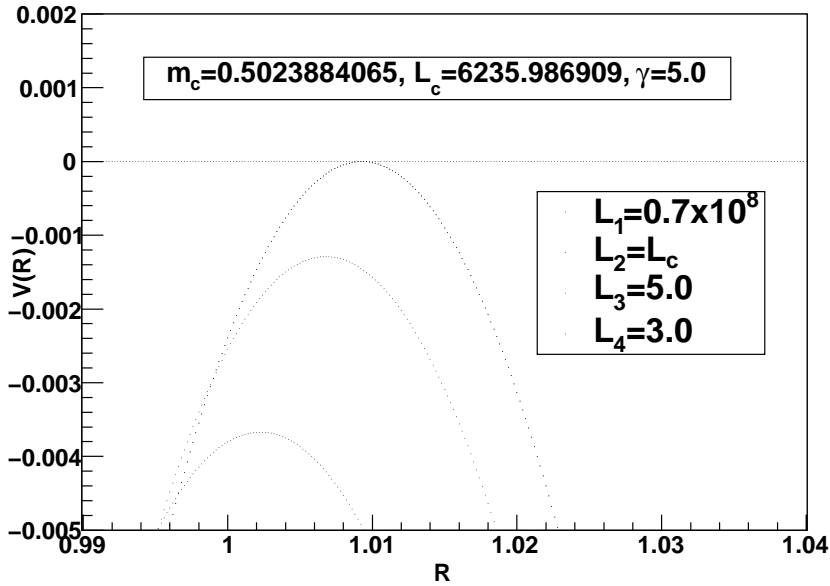


FIG. 24: The potential  $V(R)$  for  $\gamma = 5.0$ . The curves from bottom to top represent  $L_4$  to  $L_1$ , respectively, where the curves  $L_1$  and  $L_2$  coincide. Any potential curve where  $L > L_c$  will coincide with the potential curve where  $L = L_c$ .